

In vitro evolution of styrene monooxygenase from *Pseudomonas putida* CA-3 for improved epoxide synthesis

Lucas J. Gursky · Jasmina Nikodinovic-Runic ·
K. Anton Feenstra · Kevin E. O'Connor

Received: 13 May 2009 / Revised: 15 June 2009 / Accepted: 15 June 2009 / Published online: 1 July 2009
© Springer-Verlag 2009

Abstract The *styAB* genes from *Pseudomonas putida* CA-3, which encode styrene monooxygenase, were subjected to three rounds of in vitro evolution using error-prone polymerase chain reaction with a view to improving the rate of styrene oxide and indene oxide formation. Improvements in styrene monooxygenase activity were monitored using an indole to indigo conversion assay. Each round of random mutagenesis generated variants improved in indigo formation with third round variants improved nine- to 12-fold over the wild type enzyme. Each round of in vitro evolution resulted in two to three amino acid substitutions in styrene monooxygenase. While the majority of mutations occurred in *styA* (oxygenase), mutations were also observed in *styB* (reductase). A mutation resulting in the substitution of valine with isoleucine at amino acid residue 303 occurred near the styrene and flavin adenine dinucleotide binding site of styrene monooxygenase. One mutation caused a shift in the reading frame in *styA* and resulted in a StyA variant that is 19 amino acids longer than the wild-type protein. Whole cells expressing the best styrene monooxygenase variants (round 3) exhibited eight- and 12-fold improvements in styrene and indene oxidation rates compared to the wild-type enzyme. In

all cases, a single enantiomer, (*S*)-styrene oxide, was formed from styrene while (*1S,2R*)-indene oxide was the predominant enantiomer (*e.e.* 97%) formed from indene. The average yield of styrene oxide and indene oxide from their respective alkene substrates was 65% and 90%, respectively.

Keywords Biocatalysis · Directed evolution · Epoxidation · Styrene monooxygenase

Introduction

Oxidoreductase enzymes are potentially attractive biocatalysts, as they can exhibit a high degree of regio- and stereoselectivity (Li et al. 2002; van Berkel et al. 2006) and they perform reactions under mild conditions, which offer advantages over chemical processes (Archelas and Furstoss 1997; Duetz et al. 2001; van Beilen et al. 2003). Styrene monooxygenase (SMO) is a two-component NADH-dependent flavoenzyme made up of a 45-kDa oxygenase (StyA) and an 18-kDa reductase (StyB) that catalyzes the epoxidation of the vinyl side chain of styrene to form styrene epoxide (Beltrametti et al. 1997; Velasco et al. 1998; O'Leary et al. 2001; Otto et al. 2004). To date, all reports have shown that styrene monooxygenase converts styrene predominantly to (*S*)-styrene oxide (Bestetti et al. 1989; Panke et al. 1999; Hollmann et al. 2003). Previously, Panke and coworkers reported the formation of (*S*)-styrene oxide from styrene using *Escherichia coli* expressing *styAB* from *Pseudomonas putida* VLB120 with an *e.e.* of 99% (Panke et al. 2000; Park et al. 2006). Styrene monooxygenase is known to oxidize indole and conjugated alkenes to produce a range of epoxides (Di Gennaro et al. 1999; Schmid et al. 2001; Dunn et al. 2005; Feenstra et al. 2006). Indeed, a wide variety of bacteria expressing styrene

Lucas J. Gursky and Jasmina Nikodinovic-Runic made an equal contribution to the work.

L. J. Gursky · J. Nikodinovic-Runic · K. E. O'Connor (✉)
School of Biomolecular and Biomedical Sciences,
Ardmore House, and the Centre for Synthesis
and Chemical Biology, University College Dublin,
Belfield, Dublin 4, Ireland
e-mail: kevin.oconnor@ucd.ie

K. A. Feenstra
Centre for Integrative Bioinformatics VU (IBIVU),
VU University Amsterdam,
De Boelelaan 1081A, 1081HV Amsterdam, The Netherlands

monooxygenase are able to convert indole to indigo due to structural similarities between indole and styrene (O'Connor et al. 1997; O'Connor and Hartmans 1998). The rate of styrene oxide formation by a recombinant strain of *E. coli* expressing xylene monooxygenase has been reported maximally as 90 $\mu\text{mol}/\text{min}/\text{g}$ cell dry weight (Panke et al. 1999). The specific rate of indene oxide formation has not been reported. While SMO can offer advantages in terms of stereoselectivity, the rate of epoxidation reactions catalyzed by this enzyme needs to be improved to enhance the potential of SMO as a biocatalyst.

The aim of this work was to improve the rate of styrene and indene biotransformation by *E. coli* expressing SMO (from *P. putida* CA-3) through a random mutagenesis approach, namely error-prone polymerase chain reaction (PCR; directed evolution). In vitro evolution has led to a number of successes in protein engineering, resulting in improved function or stability (Bornscheuer and Pohl 2001; Farinas et al. 2001; Reetz 2001). Directed evolution requires a discriminatory screen which is often the limiting factor for strategy design. Few target substrates or products of an enzyme are colored, fluoresce, or have a convenient colorimetric assay designed for their detection (Wahler and Reymond 2001). The ability to form indigo from indole provides a convenient colorimetric method for assaying styrene monooxygenase activity and tracking its evolution over generations of random mutagenesis. There is a risk that screening for improved SMO activity toward indole will not yield an enzyme with improved activity toward styrene or indene (i.e., the evolutionary path of the enzyme is dictated by the screen) and so the selection of mutants based on the screening substrate rather than a target substrate may drive the evolution of the enzyme toward improved activity with indole but not other substrates. Given the structural similarities between indole, styrene, and indene (Fig. 1) and the convenience of the indigo formation assay, an improvement in SMO activity by screening for indigo formation was undertaken. The results of this strategy are described herein.

Materials and methods

Reagents

Indole, indene, and styrene oxide were of analytical grade and purchased from Fluka (Buchs, Switzerland). Indene oxide was purchased from Advanced Synthesis Technologies, SA (San Ysidro, CA, USA). Styrene, diethyl ether, dimethyl sulfoxide (DMSO), and acetonitrile were of gas chromatography (GC) grade and purchased from Sigma-Aldrich (Dublin, Ireland). *Pfu* Turbo DNA polymerase and T4 DNA ligase were purchased from Stratagene (La Jolla,

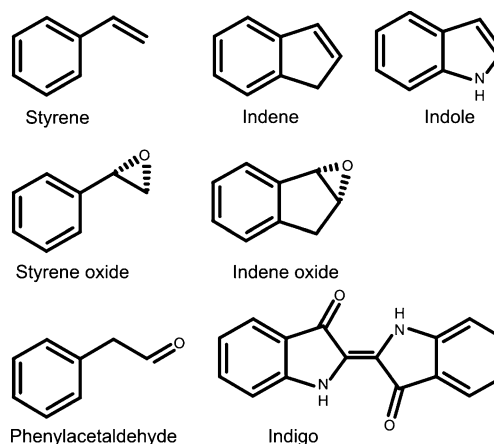


Fig. 1 Substrates (styrene, indene, indole) and products (styrene oxide, indene oxide, indole, and phenylacetaldehyde) of styrene monooxygenase biotransformations using *E. coli* BL21(DE3) cells expressing StyAB from *P. putida* CA-3

CA, USA). Restriction and DNA-modifying enzymes *Hind*III, *Xba*I, and *Nde*I were obtained from Invitrogen (Paisley, UK). Glucose, tryptone, yeast extract, casamino acids, and other media components were purchased from Sigma-Aldrich (Dublin, Ireland). Carbenicillin, isopropyl-beta-D-thiogalactopyranoside (IPTG), other salts, and reagents were purchased from Sigma (Dublin, Ireland). Oligonucleotide primers were obtained from Sigma Genosys (Dublin, Ireland). The QIAprep spin plasmid mini-prep kit, QIAEX II gel purification kit, and QIAquick PCR purification kit were purchased from QIAGEN (Hilden, Germany).

Strains, plasmids, primers, and growth conditions

Strains, plasmids, and primers used in this study are listed in Table 1. For culture propagation, Luria–Bertani (LB) complex medium or M9 minimal medium was used as described by Sambrook et al. (1989). M9 medium was supplemented with 1 ml/l of US trace element solution (1 M hydrochloric acid and the following salts, per liter: 1.50 g of $\text{MnCl}_2 \cdot 4\text{H}_2\text{O}$, 1.05 g of ZnSO_4 , 0.30 g of H_3BO_3 , 0.25 g of $\text{Na}_2\text{MoO}_4 \cdot 2\text{H}_2\text{O}$, 0.15 g of $\text{CuCl}_2 \cdot 2\text{H}_2\text{O}$, and 0.84 g of $\text{Na}_2\text{EDTA} \cdot 2\text{H}_2\text{O}$). When necessary, the medium was solidified by adding 1.5% (w/v) bacteriological agar (Difco, Detroit, USA). Alternatively, M9* mineral medium was used as described by Panke et al. (1998) which was identical to M9 minimal medium, except that it contained triple the phosphate salts and did not contain calcium chloride. Glucose was added as a carbon source to each mineral medium at a concentration of 2% (w/v), and casamino acids were added at a concentration of 0.5% (w/v). Carbenicillin (50 $\mu\text{g}/\text{ml}$) was routinely used to select for ampicillin resistance (amp^R).

Table 1 Strains, plasmids, and primers used in this study

Strain, plasmid or primer	Relevant characteristics	Source or reference
<i>Pseudomonas putida</i> CA-3	Wt, styrene degrader	O'Connor et al. (1995)
<i>E. coli</i> strains		
DH5 α	F ⁻ , <i>recA1 endA1</i> , general cloning host	Invitrogen
XL10-Gold	F ⁻ , <i>recA1, endA1, relA1</i> , cloning host	Stratagene
BL21(DE3)	F ⁻ , <i>ompT</i> , high level expression of genes regulated by T7 promoter	Novagen
Plasmids		
pBluescript II KS	Expression under <i>lac</i> promoter, amp ^R	Stratagene
pBSKS-styABR0	1.8 kbp <i>styAB</i> fragment in pBSKS, amp ^R	This work
pBSKS-styABR1	pBSKS-styABR0 derivative, positive clone from the first round of mutagenesis, amp ^R	This work
pBSKS-styABR2	pBSKS-styABR1 derivative, positive clone from the second round of mutagenesis, amp ^R	This work
pBSKS-styABR3-5	pBSKS-styABR2 derivative, positive clone from the third round of mutagenesis, amp ^R	This work
pBSKS-styABR3-10	pBSKS-styABR2 derivative, positive clone from the third round of mutagenesis, amp ^R	This work
pBSKS-styABR3-11	pBSKS-styABR2 derivative, positive clone from the third round of mutagenesis, amp ^R	This work
pRSET-B	Expression under T7 promoter, amp ^R	Invitrogen
pRSET-styABR0	pBSKS-styABR0 derivative, 1.8 kbp <i>styAB</i> fragment in pRSET-B, amp ^R	This work
pRSET-styABR1	pBSKS-styABR1 derivative, 1.8 kbp <i>styAB</i> fragment in pRSET-B, amp ^R	This work
pRSET-styABR2	pBSKS-styABR2 derivative, 1.8 kbp <i>styAB</i> fragment in pRSET-B, amp ^R	This work
pRSET-styABR3-5	pBSKS-styABR3-5 derivative, 1.8 kbp <i>styAB</i> fragment in pRSET-B, amp ^R	This work
pRSET-styABR3-10	pBSKS-styABR3-10 derivative, 1.8 kbp <i>styAB</i> fragment in pRSET-B, amp ^R	This work
pRSET-styABR3-11	pBSKS-styABR3-11 derivative, 1.8 kbp <i>styAB</i> fragment in pRSET-B, amp ^R	This work
Primers (5'–3')		
MCS F_seq	AAGTAAAACGACGGCCAGTGAAGCGCG	This work
MCS R_seq	GGAAACAGCTATGATCATGATTACGCCA	This work
StyA F_seq	CTATGTCCTTCTCGCCAGG	This work
StyA R_seq	CGAGCACCAGCGCTGTG	This work
StyB F_seq	GAACGTATCGGTCAGTGGTG	This work
StyB R_seq	CTCCGCTGGCCTTGACC	This work
KSStyAB F_HinDIII	CGCGAAGCTTAGGAGGAAGCCATGAAAAAGCGTATGG	This work
KSStyAB R_XbaI	CACATCTAGAGATCGGCACAGAAAGGCCCTC	This work
SETStyAB F_XhoI	AGGTTGCTCGAGGAAAAGCGTATCGGTATTGTTG	This work
SETStyAB R_HinDIII	ATCTTGAAGCTTCAATTCAGCGGCAACGGGTTGCC	This work

Letter in italics indicates restriction nuclease recognition sites
seq primers used for sequencing

Stock cultures of all strains used in this study were maintained at -80°C in LB broth with glycerol (20%, *v/v*). Cultures were prepared for use in experiments by inoculation of cells from frozen stock culture into broth or onto agar plates and incubated at 37°C . Cultures used to determine enzyme activities were grown at 30°C . Unless otherwise stated, cultures were induced by the addition of 1 mM (final concentration) IPTG.

Plasmid construction and StyAB in vitro evolution

Unless otherwise specified, standard recombinant DNA techniques were performed as described by Sambrook et al. (1989). Small-scale isolation of plasmid DNA from *E. coli*

was carried out by using a miniprep procedure (QIAGEN). Plasmids were transformed into electrocompetent *E. coli* cells using a Gene Pulser II (Bio-Rad, Hercules, CA, USA) according to the manufacturer's instructions. For the random mutagenesis experiments, *E. coli* XL-10 Gold ultracompetent cells were used and transformed according to the manufacturer's instructions (Stratagene 2005).

The *styAB* fragment from *P. putida* CA-3 was amplified from chromosomal DNA template using primers KSStyAB F_HinDIII and KSStyAB R_XbaI (Table 1). PCR was done on a DNA Engine Thermal Cycler (Bio-Rad, Hercules, CA, USA) using the following method: 94°C for 1 min; 30 cycles of 94°C for 30 s, 55°C for 30 s, and 72°C for 2 min; and a final extension at 72°C for 10 min. The 1.8-

kbp fragment generated by PCR was digested with *HinDIII* and *XbaI* and ligated into pBluescript KS to generate pBSKS-StyABR0 (Table 1). Similarly, all other recombinant vectors were generated using appropriate primers and restriction sites (Table 1). To verify plasmid constructs, DNA sequencing was conducted by GATC Biotech (Hamburg, Germany) using appropriate primers. Sequence data were aligned and compared using Sequencher 4.7, using the default alignment settings (Gene Codes Corp., Ann Arbor, MI, USA). Sequencing data have been submitted under the GenBank accession number EU155061.

In vitro evolution of *styAB* was performed using a GeneMorph II EZClone Random Mutagenesis Kit (Stratagene, La Jolla, CA, USA) according to the manufacturer's instructions. Briefly, mutant megaprimer synthesis was carried out by error prone PCR amplification of *styAB* fragment from the pBSKS-StyAB0 vector for the first round of mutagenesis. For all subsequent rounds, plasmid template for the megaprimer synthesis was isolated from mutants of the previous round of mutagenesis identified as indigo producing by assay and sequence verification. The megaprimers were synthesized by 30 cycles of PCR (as above) using 1,000 ng of purified plasmid template for round 1 (low mutation frequency), 200 ng for round 2 (medium mutation frequency), and 100 ng for round 3 (high mutation frequency).

The megaprimers generated during the PCR reaction were subsequently used to amplify the rest of the plasmid using high fidelity DNA polymerase, thus generating the library of recombinant plasmids with mutations introduced within the *styAB* fragment. The resulting plasmids from each round of mutagenesis were used to transform XL-10 Gold ultracompetent cells, which were then plated on LB agar plates containing carbenicillin (50 µg/ml), indole (1 mM), and IPTG (1 mM) and grown for 16 h at 37°C.

Screening for *styAB* gene variants encoding enzymes with indigo production activity

Libraries of variants generated by each round of directed evolution were screened for improved indigo production rates. Colonies grown on LB agar plates containing carbenicillin (50 µg/ml), indole (1 mM), and IPTG (1 mM) were visually screened for most rapid blue color (indigo) production. Single colonies chosen for further screening were grown in 200 µl M9 broth supplemented with carbenicillin (50 µg/ml) and IPTG (1 mM) for 24 h at 37°C in a 96-well microtiter plate. Each microtiter plate contained uninoculated wells as a negative control, while the parent strain (from the previous generation) was used as a positive control. Following 24 h of growth, the absorbance of each well in the 96-well plate was measured

at 600 nm to obtain the cell culture density before the plate was centrifuged (3,000×g) at 30°C for 15 min and the supernatant removed by vacuum aspiration. The pelleted cells were resuspended in 100 µl of 50 mM potassium phosphate buffer (pH 7) containing 1 mM indole. Cell resuspensions were incubated for 1 to 4 h at 30°C with shaking at 200 rpm. The protocol for spectrophotometric monitoring of indigo formation was adapted from that described previously (O'Connor et al. 1997), to allow for easier screening in the microtiter plates. Following incubation with indole, 200 µl of DMSO was added to each well and incubated for 5 min at room temperature to lyse the cell cultures and terminate the reaction. The assay plate was then centrifuged (3,000×g) in a benchtop centrifuge with swinging buckets adapted for MT plate for 10 min, and 200 µl of the supernatant was transferred to a new 96-well plate. The absorbance at 610 nm was determined for all wells. The negative control values were averaged and subtracted from the values obtained for each test well. Cultures showing increased indigo formation greater than the positive control were selected for further screening and confirmation of increased activity. Cultures which exhibited improved rates of indigo formation were grown in LB broth supplemented with carbenicillin and frozen as stock cultures. Recombinants with the highest rates of indigo formation were cultured for plasmid isolation and sequenced (GATC Biotech, Hamburg, Germany). The recombinant with the greatest increase in indigo formation rate was chosen as the parental strain for the next round of directed evolution.

Whole-cell biotransformations: determination of substrate depletion and product formation rates by *E. coli* cells expressing styrene monooxygenase

SMO activity was determined by a whole-cell assay as described by Panke et al. (1998). *E. coli* XL-10 Gold cells expressing *styAB* from pBluescript were used during the screening phase of the in vitro evolution. To enhance expression of styrene monooxygenase, the *styAB* genes were subcloned into pRSETB and transformed into *E. coli* BL21(DE3) cells (Table 1).

E. coli cells were grown in M9* mineral medium (3 ml; supplemented with glucose, casamino acids, carbenicillin, and US trace element solution) at 30°C for 16 h and then inoculated into larger cultures (250 ml; 0.2% inoculum) and grown in an identical medium at 30°C with shaking at 200 rpm. Once the culture had reached an optical density of 0.5 (600 nm; Helios Gamma UV-visible spectrophotometer, Thermo Scientific), the cells were induced with 1 mM IPTG and further incubated for 12–14 h. The cells were then harvested by centrifugation at 3,000×g for 20 min (Benchtop 5810R; Eppendorf) and resuspended to a

concentration of 0.5 g CDW/l in 100 mM potassium phosphate buffer (pH 7.4) containing 1% (w/v) glucose. Aliquots of 2 ml were distributed into 15 ml Pyrex tubes and incubated horizontally on a rotary shaker at 200 rpm. After 5 min, the substrate was added to a final concentration of 1.5 mM from a 30-mM stock solution in ethanol. The reaction continued at 30°C for 60 min with shaking at 200 rpm and was stopped at various time points (one vial per time point) by immediate addition of ice-cold ether (2 ml; containing 0.1 mM 1-dodecanol as an internal GC standard) and incubating the sample on ice. After addition of saturating amounts of sodium chloride, the water phase was extracted by vigorous shaking at 30°C for 5 min, and the phases were separated by centrifugation at 3,000×g at 4°C for 5 min. The organic phase was analyzed by gas chromatography. Indole depletion was monitored as previously described (O'Connor et al. 1997) and indigo formation was monitored spectrophotometrically as described above.

Protein expression analysis

The pRSET-derived expression constructs (Table 1) encoded his6::*styAB* fusion as this would allow to rapidly assess protein expression through Western blotting. To test the level of expression of the His-tagged protein, *E. coli* BL21(DE3) cultures harboring pRSET-*styAB* constructs were grown and treated as described for the whole-cell biotransformation experiments (cells harvested, washed in 50 mM phosphate buffer pH 7.0, and resuspended in 50 mM phosphate buffer pH 7 to a concentration of 0.5 g CDW/l). One milliliter of cell suspension was used for the Western blot analysis. Cells (0.5 g CDW/l) were centrifuged and resuspended in 1 ml of BugBuster solution containing benzonase (2 U/ml; Novagen) and incubated at 30°C for 15 min with shaking (200 rpm). Soluble proteins were separated by sodium dodecyl sulfate polyacrylamide gel electrophoresis (SDS-PAGE; 10%, w/v) and transferred to a nitrocellulose membrane (Hybond ECL; Amersham Biosciences). The membrane was probed with Penta-His HRP conjugate antibody (Qiagen, Hilden, Germany). The blot was developed using Immobilon™

Western chemiluminescent HRP substrate according to the manufacturer's protocol (Millipore, Ireland). Immunoluminescence was detected and evaluated using chemiluminescence compatible FluorChem™ imaging system equipped with AlphaEase FC2 software (Alpha Innotech, San Leandro, CA, USA).

Analytical procedures

Gas chromatography was used for separation of styrene, styrene oxide, indene and indene oxide. A Fison 8000 series GC equipped with an Agilent HP-1 capillary column (30 m, 0.25 mm inner diameter, 0.25 μm film thickness; J&W Scientific, USA) was used with splitless injection and hydrogen as the carrier gas. A temperature gradient of 50–180°C was implemented with an increment of 10°C/min. Detection was done using a flame ionization detector. Alternatively, a Supelco Beta-DEX 120 column (30 m, 0.25 mm inner diameter, 0.25 mm film thickness; Supelco, Buchs, Switzerland) was used with splitless injection and an isothermal oven temperature profile at 90°C for separation of styrene oxide enantiomers as described previously (Panke et al. 1998). Compounds were identified by comparison of retention times with commercially available standards. High-performance liquid chromatography analysis of indole depletion was performed using a Hypersil C-18 column ODS 5 μm column (125×3 mm; Hypersil, Runcorn, UK) and a Hewlett Packard HP1100 instrument equipped with an Agilent 1100 Series diode array detector. The samples were isocratically eluted using an acetonitrile and water mix (1:1) at a flow rate of 0.5 ml/min.

Styrene monooxygenase structure analysis modeling

Mutated positions in the StyA protein were mapped onto the available homology model structure (PDB id. 2HD8; Feenstra et al. 2006). Minimal atomic distances between mutated residues and the styrene substrate and flavin adenine dinucleotide (FAD) cofactor in the model structure were determined using the *g_mindist* tool from Gromacs 3.3.3 (Lindahl et al. 2001).

Table 2 Indigo formation rates for *E. coli* XL-10 Gold cells expressing wild type and variant styrene monooxygenase generated through error prone PCR of *styAB*

Variant name	Mutagenesis round	Indigo formation rate (μmol/min/g CDW)	Fold Improvement	Cumulative improvement
Wild type (R0)	0	2.1	0.0	0.0
R1	1	11.3	5.4	5.4
R2	2	17.2	1.5	8.2
R3-5	3	26.5	1.5	12.6
R3-10	3	20.6	1.2	9.4
R3-11	3	18.6	1.1	8.9

Results

Screening for improved styrene monooxygenase using the indole-to-indigo assay

A mutant library of the 1.8-kb *styAB* gene was created using GeneMorph II EZClone random mutagenesis kit as described in “Plasmid construction and StyAB in vitro evolution” section. *E. coli* XL-10 Gold cells expressing styrene monooxygenase on pBluescript (pBSKS-*styAB*) were using during the screening phase of in vitro evolution. Of the 1,032 *E. coli* clones screened in round 1, a *styAB* variant with a 5.4-fold improvement in the rate of indigo formation compared to the wild-type enzyme was selected for further mutagenesis (Table 2). *E. coli* cells expressing the best round 2 variant (R2) exhibited a 1.5-fold higher indigo formation rate compared to variant R1. A number of variants generated in the third round of random mutagenesis showed improved rates of indigo formation over the round 2 mutant and represents a nine- to 12-fold improvement in activity for round 3 variants for indigo formation compared to the wild-type styrene monooxygenase (Table 2).

Sequencing of 15 randomly selected clones from the mutant library revealed that the mutation frequency of the library was 3.2 nucleotides per gene and that each round of in vitro evolution resulted in two to three amino acid (AA) substitutions when compared to wild-type *P. putida* CA-3 (data not shown). The mutations introduced in any one round of mutagenesis were maintained in the StyAB sequence in subsequent mutagenesis rounds (Fig. 2).

Identification of mutations in styrene monooxygenase variants

In round 1 of the random mutagenesis, two mutations occurred in StyA (F88L and K150R) and a single mutation (N150S) within the reductase StyB. During the second round of in vitro mutagenesis, an insertion of 8 bp (ACTATTGC) occurred near the C-terminal region of *styA* (nucleotide position 1242). This insertion is a direct repeat of the 8 bp preceding the insertion. The 5-bp repeat ATTGC occurs three times in the same region (nucleotide position 1242–1386) in the wild-type gene. This insertion resulted in a change of the translational reading frame and subsequently resulted in a predicted protein 19 AAs longer than the wild-type oxygenase (StyA). This 19 AA “tail” has the sequence: LRPDAIAPLVKASGALTPG. In addition to the tail, a substitution A415L also occurred within StyA. The frameshift did not affect the start codon or reading frame of *styB*. The substitution E124D was also introduced within StyB in the second round of mutagenesis (Fig. 2). The third round of random mutagenesis produced three additional variants worthy of further

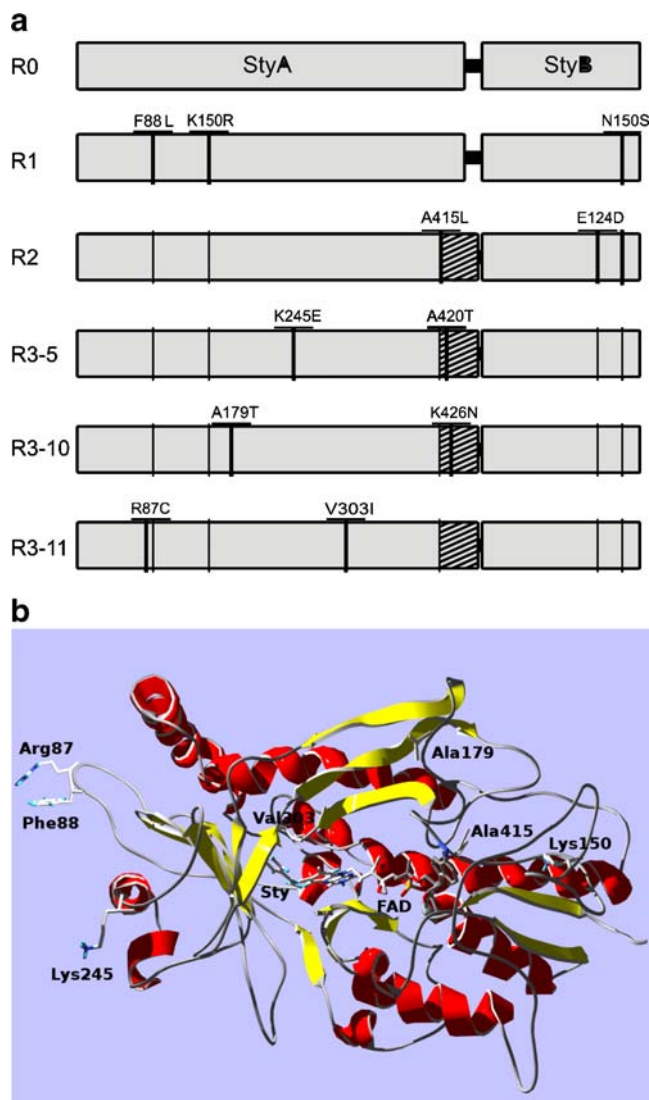


Fig. 2 **a** Schematic diagram of mutations introduced into styrene monooxygenase (StyAB) through error prone PCR and **b** molecular model of the styrene monooxygenase (StyA) catalytic domain highlighting various amino acid residues that were substituted. The following amino acid substitutions occurred in comparison to wild-type StyAB (R0): F88L, K150R within StyA, and N150S within StyB in variant R1; A415L within StyA and E124D within StyB in variant R2; K245E and A420T within StyA in variant R3_5; A179T and K426N within StyA in variant R3_10; and R87C and V303I within StyA of variant R3_11. Shaded area is an additional 19 amino acid “tail” that was introduced from variant R2 due to insertion causing the frameshift mutation

examination. In variant R3-11 (R87C), an amino acid change occurs in StyA at the residue just preceding the mutation found in variant R1 (F88L) from round 1 and a substitution V303I in the amino acid just following the GDX₆P motif. Variants R3-5 and R3-10 both contain two mutations each in *styA*, one of which occurs in the extra N-terminal “tail” added on by the frameshift from round 2 for each mutant (Fig. 2).

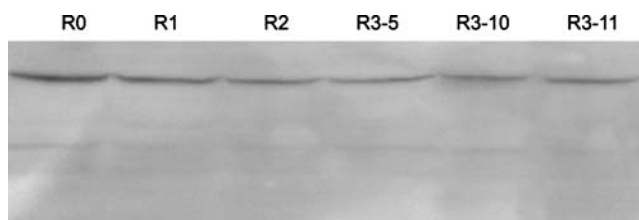


Fig. 3 Western blot analysis of the cell lysates of *E. coli* BL21(DE3) cells expressing the wild-type StyAB (R0) and StyAB variants (R1, R2, R3-5, R3-10, and R3-11). Fifteen microliters of *E. coli* cell lysate from each sample containing 0.35 mg ml⁻¹ of protein was loaded in each well

Styrene and indene biotransformations: rates, stoichiometry, and enantiomeric excess

While screening for indigo formation allowed us to select mutants with higher styrene monooxygenase activity (expressed in pBluescript II KS), the aim of this study was to generate whole-cell biocatalysts with enhanced epoxide synthesizing capability. To maximize the expression of styrene monooxygenase, the *styAB* genes were subcloned into the high expression vector pRSETB (based on T7 promoter) and transformed into *E. coli* BL21(DE3) cells (Table 1). As our attempts to purify the SMO were unsuccessful (data not shown), the expression level of SMO wild type and variants in *E. coli* BL21(DE3) cells were compared using SDS-PAGE analysis of the cell lysates and the His tag antibody specific for histidine-tagged proteins (Fig. 3). Using chemiluminescence detection, a single band was observed in the cell lysates. Using densitometry software, wild-type (R0) expression levels were found to be slightly higher (2–7%) in comparison to the variants (Fig. 3).

E. coli BL21(DE3) cells expressing variant R1 consumed styrene and indene 3.2- and 1.6-fold higher than cells expressing the wild-type enzyme, respectively. The rate of styrene and indene consumption by cells expressing styrene monooxygenase round 2 variant decreased 1.6- and 3.2-fold, respectively. Round 3 of error-prone PCR generated variants of *styAB* (R3-5, R3-10, R3-11) with eight- to 12-fold

increased styrene and indene transformation rates compared to cells expressing the wild-type enzyme (Table 3). The ratio of styrene to indene consumption by wild-type StyAB is 1.14:1. However, the ratio of styrene to indene consumption for R3-10 is 1:1.3, and thus, the evolution of this enzyme is toward indene epoxidation rather than styrene epoxidation. Conversely, variant R3-11 has evolved toward styrene oxidation with a ratio of 2:1 for styrene to indene consumption (Table 3). In general, a linear relationship between alkene (e.g., styrene and indene) consumption and epoxide formation occurs for *E. coli* cells expressing styrene monooxygenase (*styAB*) between 5 and 60 min, depending upon the variant used in the biotransformation (Figs. 4 and 5).

The best SMO variant (R3-10) consumed 1.4 mM styrene completely within 15 min. The rate of styrene consumption dropped sharply after 5 min once the concentration of styrene fell below 0.11 mM. The maximum amount of styrene oxide was observed after 5 min (Fig. 4). In styrene biotransformations, (*S*)-styrene oxide was the only enantiomer detected by chiral GC analysis. In all biotransformations with styrene, approximately 65% product appeared as styrene oxide (66.25% (R0), 69.7% (R1), 65% (R2), 64.5% (R3-10)). The remaining product (30–35%) appears as phenylacetaldehyde in styrene biotransformations (data not shown).

The transformation of indene by cells expressing *styAB* produced a single product: indene oxide. Between 88.2% and 94.5% of utilized indene appeared as indene oxide in biotransformations. In the best variant (R3-10), the rate of indene transformation is the fastest within the first 5 min and slows dramatically after this time point, with indene oxide appearance following the same pattern (Fig. 5). (*1S,2R*)-Indene oxide is the predominant enantiomer formed from indene biotransformation, with an *e.e.* of 97%.

Discussion

The in vitro evolution of *styAB* from *P. putida* CA-3 has generated new styrene monooxygenase variants that oxidize

Table 3 Initial rates (μmol/min/g CDW) of substrate utilization and product formation by *E. coli* BL21 (DE3) cells expressing wild type and variants of styrene monooxygenase (pRSET-styAB)

Variant	Styrene consumption	Styrene oxide formation	Indene consumption	Indene oxide formation
R0	53±0.1	21±0.7	47±0.1	37±0.1
R1	169±1	75±0.5	74±0.8	49±0.3
R2	53±0.5	20±0.2	46±0.4	30±0.7
R3-5	336±2	182±1	370±1	327±1
R3-10	421±1	266±2	546±2	434±4
R3-11	418±1	252±2	206±1	175±2

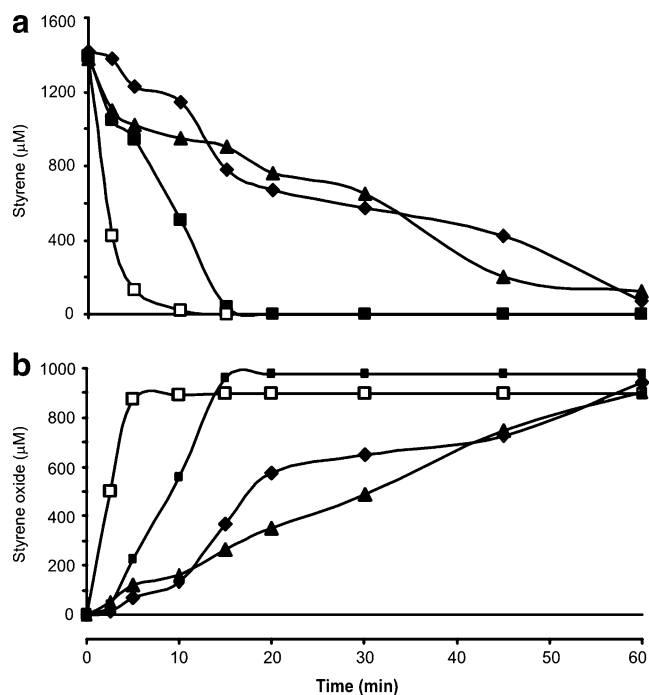


Fig. 4 Styrene depletion (a) and styrene oxide formation (b) by *E. coli* BL21(DE3) cells expressing wild-type StyAB (RO, closed diamond) and selected variants (closed square R1, closed triangle R2, open square R3-10)

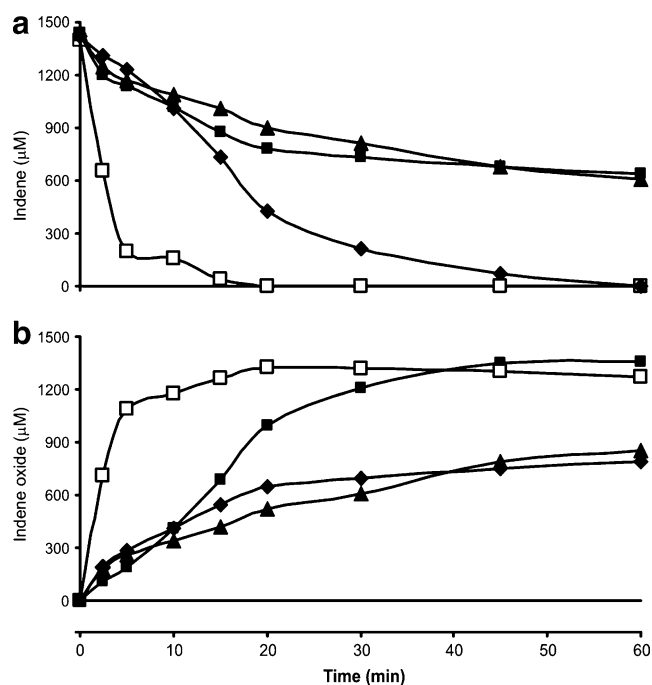


Fig. 5 Indene depletion (a) and indene oxide formation (b) over time by *E. coli* BL21(DE3) cells expressing StyAB wild type (RO, closed diamond) and selected variants (closed square R1, closed triangle R2, open square R3-10)

Table 4 Distances (Ångström) between atoms of mutated residues in styrene monooxygenase and the binding pockets of styrene and FAD

Amino acid residue	Distance from FAD (Å)	Distance from styrene (Å)
R87	35.2	28.0
F88	32.4	25.3
K150	11.1	29.3
A179	9.1	24.8
K245	19.6	17.5
V303	6.2	4.0
A415	13.8	20.3

styrene and indene at rates higher than the wild-type enzyme. Round 3 variants R3-10 and R3-11 utilized styrene at a rate eightfold higher than cells expressing wild type enzyme (R0). Variant R3-10 also exhibited the highest rate of indene utilization (Table 3) which is 12-fold higher than that exhibited by cells expressing the wild type enzyme. Variant R3-10 generated herein exhibit a 35-fold higher rate of indene oxide formation than that reported for SMO from *P. putida* VLB120 expressed in *E. coli* cells (12.5 $\mu\text{mol}/\text{min}/\text{g}$ CDW; Schmid et al. 2001). Thus, the rate of styrene oxide and indene oxide formation by *E. coli* cells expressing *P. putida* CA-3 styrene monooxygenase variants is the highest reported for any biocatalyst (Panke et al. 1998, 2000; Park et al. 2006).

(*S*)-Styrene oxide was the only enantiomer detected by chiral GC analysis using wild type and variants of styrene monooxygenase. This is in accordance with previous reports for SMO expressed in *E. coli* which shows an *e.e.* greater than 99% (Panke et al. 1998, 1999). The oxidation of styrene by styrene monooxygenase did not result in a single product as phenylacetaldehyde was also detected.

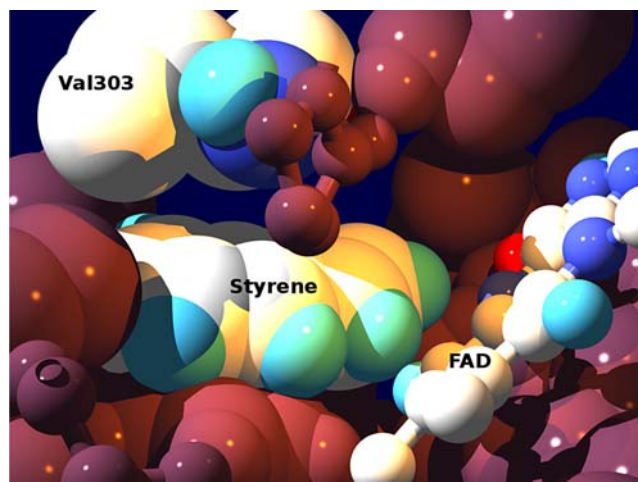


Fig. 6 Styrene monooxygenase active site region with the valine residue at position 303 and its neighboring residues

Panke and coworkers reported the formation of 2-phenylethanol as a byproduct of styrene transformation by *E. coli* cells expressing SMO from *P. putida* VLB120 (Panke et al. 1998). Based on the work of Beltrametti and coworkers, Panke suggested that a pinacol-type rearrangement of styrene oxide could occur to form phenylacetaldehyde (Beltrametti et al. 1997; Panke et al. 1998). The *e.e.* of (*IS-2R*) indene oxide of 97% was marginally lower than that for styrene oxide but the former appeared as a single product and the yield from indene was 1.4-fold higher than the yield of styrene oxide from styrene. A similar *e.e.* for indene oxide is reported by Schmidt et al. using *E. coli* JM101 (pSPZ10) expressing SMO from *P. putida* VLB120 (Schmid et al. 2001).

A number of mutations occurred in both StyA and StyB. Identified mutations were mapped onto the homology model of StyA to analyze the molecular basis of their effects (Fig. 2b; Feenstra et al. 2006). The distances between the mutated residues and the binding pockets in the protein for styrene and FAD are listed in Table 4. Only one mutation is located at near atomic contact (less than 6 Å) from the styrene and FAD binding site, i.e., V303I (Fig. 6). The mutation at residue 303 occurs just after a conserved GDX₆P motif, which has been shown to have dual function in FAD/NAD(P)H binding in flavoprotein hydroxylases (Eppink et al. 1997). The V303 side chain is an integral part of the substrate binding cavity, and its backbone nitrogen, together with that of P302, is implicated to play a role in the catalytic mechanism (Ridder et al. 2000; Feenstra et al. 2006). The close interaction between V303 and styrene allows us to postulate the effects of the mutation (V303I) on the catalytic rates for styrene and indene. Isoleucine is only one methyl group bigger than valine, but as the area around position 303 is neatly packed, this methyl will probably point into the substrate cavity, restricting the space in the cavity. In addition, indene contains an additional methylene group compared to styrene (Fig. 1). We can hypothesize that either indene, the transition state, or the product does not fit as well in the binding pocket with the bigger isoleucine present at the active site. This could explain the relatively low rate for indene compared to styrene in the R3-11 variant (Tables 3 and 4).

The extended C-terminal “tail” that first appears in R2 is maintained throughout all of the R3 variants. The tail may help to maintain a closer interaction between the StyA and StyB proteins, or possibly enable a more efficient electron/proton transfer. However, previous reports have shown that StyA and StyB do not interact, and thus, the promotion of more efficient electron/proton transfer is more likely (Otto et al. 2004; Kantz et al. 2005). Other amino acid changes occur throughout StyAB such as A179T and K245N in variant R3-10 which exhibits a higher activity toward indene compare to styrene but it is difficult to predict the

exact effect of these amino acid changes as they appear to be far from the active site. Nevertheless, previous studies have found that a large number of mutations occur outside the active site of enzymes that have been improved through random mutagenesis (Bornscheuer and Pohl 2001; Farinas et al. 2001; Glieder et al. 2002) indicating that complex effects of amino acid changes that are difficult to model and predict can dramatically affect enzyme activity.

Single-component monooxygenases and hydroxylases generally do not share a high degree of sequence similarity (Harayama et al. 1992). However, the conserved glycine motif (sequence GXGXXG) found at residues 9 to 14 within the N-terminal region of StyA are postulated to play an important role in FAD binding (Hofsteenge et al. 1980; Feenstra et al. 2006). These residues were not observed to have undergone any mutational alterations in the mutants generated in this study. Mutations in this conserved motif would very likely lead to inactive variants, and hence, no variants bearing mutations here could be found.

The use of the indole to indigo screen has proven useful for the selection of variant enzymes that exhibit higher rates of epoxide formation. However, given that the variants generated in round 2 exhibited higher rates of indigo formation but lower rates of styrene oxide and indene oxide formation, the risk of generating a variant with improved activity toward the screening substrate and not the target substrate exists with this strategy.

In conclusion, the random mutation of styrene monooxygenase using error prone PCR has generated a number of improved variants exhibiting the highest known rate of (*S*)-styrene epoxide and (*IS-2R*) indene epoxide production by a biocatalyst.

Acknowledgments This work was supported by the Science Foundation Ireland (grant no. 04/IN3/B581). We thank Dr. Derek Boyd and Dr. Narain Sharma, Queens University Belfast, for the synthesis of *IS-2R*-indene oxide.

References

- Archelas A, Furstoss R (1997) Synthesis of enantiopure epoxides through biocatalytic approaches. *Annu Rev Microbiol* 51:491–525
- Beltrametti F et al (1997) Sequencing and functional analysis of styrene catabolism genes from *Pseudomonas fluorescens* ST. *Appl Environ Microbiol* 63:2232–2239
- Bestetti G, Galli E, Benigni C, Orsini F, Pelizzioni F (1989) Biotransformations of styrenes by a *Pseudomonas putida*. *Appl Microbiol Biotechnol* 30:252–256
- Bornscheuer UT, Pohl M (2001) Improved biocatalysts by directed evolution and rational protein design. *Curr Opin Chem Biol* 5:137–143
- Di Gennaro P, Colmegna P, Galli E, Sello G, Pelizzioni F, Bestetti G (1999) A new biocatalyst for production of optically pure aryl epoxides by styrene monooxygenase from *Pseudomonas fluorescens* ST. *Appl Environ Microbiol* 65:2794–2797

- Duetz WA, van Beilen JB, Witholt B (2001) Using proteins in their natural environment: potential and limitations of microbial whole-cell hydroxylations in applied biocatalysis. *Curr Opin Biotechnol* 12:419–425
- Dunn HD et al (2005) Aromatic and aliphatic hydrocarbon consumption and transformation by the styrene degrading strain *Pseudomonas putida* CA-3. *FEMS Microbiol Lett* 249:267–273
- Eppink MH, Schreuder HA, Van Berkel WJ (1997) Identification of a novel conserved sequence motif in flavoprotein hydroxylases with a putative dual function in FAD/NAD(P)H binding. *Protein Sci* 6:2454–2458
- Farinas ET, Bulter T, Arnold FH (2001) Directed enzyme evolution. *Curr Opin Biotechnol* 12:545–551
- Feenstra AK, Hofstetter K, Bosch R, Schmid A, Commandeur JNM, Vermeulen NPE (2006) Enantioselective substrate binding in a monooxygenase protein model by molecular dynamics and docking. *Biophys J* 91:3206–3216
- Glieder A, Farinas ET, Arnold FH (2002) Laboratory evolution of a soluble, self-sufficient, highly active alkane hydroxylase. *Nat Biotechnol* 20:1135–1139
- Harayama S, Kok M, Neidle EL (1992) Functional and evolutionary relationships among diverse oxygenases. *Annu Rev Microbiol* 46:565–601
- Hofsteenge J, Vereijken JM, Weijer WJ, Beintema JJ, Wierenga RK, Drenth J (1980) Primary and tertiary structure studies of p-hydroxybenzoate hydroxylase from *Pseudomonas fluorescens*. *Eur J Biochem* 113:141–150
- Hollmann F, Lin P-C, Witholt B, Schmid A (2003) Stereospecific biocatalytic epoxidation: the first example of direct regeneration of a FAD-dependent monooxygenase for catalysis. *J Am Chem Soc* 125:8209–8217
- Kantz A, Chin F, Nallamothu N, Nguyen T, Gassner GT (2005) Mechanism of flavin transfer and oxygen activation by the two-component flavoenzyme styrene monooxygenase. *Arch Biochem Biophys* 442:102–116
- Li Z et al (2002) Oxidative biotransformations using oxygenases. *Curr Opin Chem Biol* 6:136–144
- Lindahl E, Hess B, van der Spoel D (2001) GROMACS 3.0: a package for molecular simulation and trajectory analysis. *J Mol Model* 7:306–317
- O'Connor KE, Hartmans S (1998) Indigo formation by aromatic hydrocarbon-degrading bacteria. *Biotechnol Lett* 20:219–223
- O'Connor KE, Buckley CM, Hartmans S, Dobson ADW (1995) Possible regulatory role for nonaromatic carbon sources in styrene degradation by *Pseudomonas putida* CA-3. *Appl Environ Microbiol* 61:544–548
- O'Connor KE, Dobson ADW, Hartmans S (1997) Indigo formation by microorganisms expressing styrene monooxygenase activity. *Appl Environ Microbiol* 63:4287–4291
- O'Leary ND, O'Connor KE, Duetz W, Dobson ADW (2001) Transcriptional regulation of styrene degradation in *Pseudomonas putida* CA-3. *Microbiol* 147:211–218
- Otto K, Hofstetter K, Rothlisberger M, Witholt B, Schmid A (2004) Biochemical characterization of StyAB from *Pseudomonas* sp. strain VLB120 as a two-component flavin-diffusible monooxygenase. *J Bacteriol* 186:5292–5302
- Panke S, Witholt B, Schmid A, Wubbolts MG (1998) Towards a biocatalyst for (S)-styrene oxide production: characterization of the styrene degradation pathway of *Pseudomonas* sp. strain VLB120. *Appl Environ Microbiol* 64:2032–2043
- Panke S, Meyer A, Huber CM, Witholt B, Wubbolts MG (1999) An alkane-responsive expression system for the production of fine chemicals. *Appl Environ Microbiol* 65:2324–2332
- Panke S, Wubbolts MG, Schmid A, Witholt B (2000) Production of enantiopure styrene oxide by recombinant *Escherichia coli* synthesizing a two-component styrene monooxygenase. *Biotechnol Bioeng* 69:91–100
- Park J-B et al (2006) The efficiency of recombinant *Escherichia coli* as biocatalyst for stereospecific epoxidation. *Biotechnol Bioeng* 95:501–512
- Reetz MT (2001) Combinatorial and evolution-based methods in the creation of enantioselective catalysts. *Angew Chem Int Ed* 40:284–310
- Ridder L, Mulholland AJ, Rietjens I, Vervoort J (2000) A quantum mechanical/molecular mechanical study of the hydroxylation of phenol and halogenated derivatives by phenol hydroxylase. *J Am Chem Soc* 122:8728–8738
- Sambrook J, Fritsch EF, Maniatis T (1989) *Molecular cloning: a laboratory manual*. Cold Spring Harbor Laboratory, Cold Spring Harbor
- Schmid A, Hofstetter K, Feiten H, Hollmann F, Witholt B (2001) Integrated biocatalytic synthesis on gram scale: the highly enantioselective preparation of chiral oxiranes with styrene monooxygenase. *Adv Synth Catal* 343:732–737
- Stratagene (2005) *GeneMorph II random mutagenesis kit: instruction manual*. Stratagene, La Jolla
- van Beilen JB, Duetz WA, Schmid A, Witholt B (2003) Practical issues in the application of oxygenases. *Trends Biotechnol* 21:170–177
- van Berkel WJH, Kamerbeekb NM, Fraaije MW (2006) Flavoprotein monooxygenases, a diverse class of oxidative biocatalysts. *J Biotechnol* 124:670–689
- Velasco A, Alonso S, Garcia JL, Perera J, Diaz E (1998) Genetic and functional analysis of the styrene catabolic cluster of *Pseudomonas* sp. strain Y2. *J Bacteriol* 180:1063–1071
- Wahler D, Reymond J-L (2001) Novel methods for biocatalyst screening. *Curr Opin Chem Biol* 5:152–158